DOI: 10.1002/chem.200501404

Controlled Hydrothermal Synthesis and Growth Mechanism of Various Nanostructured Films of Copper and Silver Tellurides

Lizhi Zhang,*[a] Zhihui Ai,[a] Falong Jia,[a] Li Liu,[a] Xianluo Hu,[b] and Jimmy C. Yu*[b]

Abstract: Various nanostructured films of copper and silver tellurides were hydrothermally grown on the corresponding metal substrates through reactions between metal foils and tellurium powder in different media. Interesting morphologies including nanowires, nanorods, nanobelts, nanosheets, and hierarchical dendrites were obtained. The nanostructured films were characterized by using X-ray diffraction (XRD), scanning electron microscopy (SEM), transmission electron microscopy (TEM), and high-resolution TEM (HRTEM). A growth mechanism was proposed based on the characterization results. This study provides a low-temperature, solution-phase approach to grow low-dimensional, nanostructured metal tellurides with controllable morphologies.

Keywords: copper · hydrothermal synthesis · nanostructures · silver · tellurium

Introduction

Transition-metal nanocrystalline chalcogenides have attracted much attention over the past years because of their interesting properties and many potential applications.[1,2] Among them, tellurides are attractive materials for thermoelectric applications owing to their very high thermopower values and the fact that both *p*- and *n*-type materials can be obtained by doping.[3] For instance, silver telluride alloys possess interesting thermoelectrical, electrical, and magnetoresistive properties and find wide applications in the fields of thermoelectronics, magnetics, and sensors. The low-temperature phase of monoclinic silver telluride is a semiconductor with a narrow band gap, high carrier mobility, and low lattice thermal conductivity, whereas its high-temperature phase gives rise to superionic conductivity.[4] A large positive magnetoresistance effect has also been observed in both Ag- (*n*-type) and Te-rich (*p*-type) silver telluride.[5–7] Copper telluride thin films have many applications in various devices such as solar cells, superionic conductors, photodetectors, photothermal conversion, electroconductive electrodes, microwave-shielding coatings, and so forth.[8–10]

Traditionally, metal tellurides have been synthesized by an elemental reaction at elevated temperatures, typically 500–600 °C, in evacuated tubes,[11] or by the reaction of aqueous metal–salt solutions with a toxic and malodorous gas H_2Te,[12] or by mechanical alloying from elemental powders.[13] Parkin and co-workers reported a room-temperature route to synthesize Ag and Cu chalcogenides in liquid ammonia.[14] Most of the products Parkin obtained were amorphous and usually crystallized after thermal treatment at 300 °C.[15] During Parkin's experiments, manipulations had to be carried out very carefully at −77 °C in thick-walled glass vessels. Qian and co-workers synthesized copper and silver chalcogenides by using solvothermal methods at temperatures in the range 140–180 °C. The products were usually formed as nanoparticles.[16,17]

Low-dimensional nanostructures, including nanowires, nanorods, and nanosheets, are of importance because they may exhibit promising mechanical, electrical, optical, and magnetic properties different from those of their corresponding polycrystalline powders. These low-dimensional materials have potential applications in molecular-based electronic devices such as optical memories, switches, displays, and data records.[18] Until now, there have been few studies on low-dimensional nanostructures of silver tellurides, such as silver telluride nanowire arrays synthesized by

[a] Prof. L. Zhang, Dr. Z. Ai, Dr. F. Jia, L. Liu
Key Laboratory of Pesticide & Chemical Biology
Ministry of Education, College of Chemistry
Central China Normal University
Wuhan, 430079 (China)
Fax: (+86) 27-6786-7535
E-mail: zhanglz@mail.ccnu.edu.cn

[b] X. Hu, Prof. J. C. Yu
Department of Chemistry
The Chinese University of Hong Kong
Shatin, New Territories, Hong Kong (China)
Fax: (+852) 2603-5057
E-mail: jimyu@cuhk.edu.hk

cathodic electrolysis into porous anodic alumina membranes.[19,20] To the best of our knowledge, low-dimensional copper telluride nanostructures have not been synthesized.

Recently, we have developed a general solution-phase strategy to grow nanostuctured metal chalcogenides through hydrothermal reaction of metal foils with chalcogen powders. Lead telluride nanotubes and nanowires on lead foils and oriented nanostructured nickel sufides on nickel foils have been reported.[21,22] Herein we report that various nanostructured copper and silver telluride films can be controllably obtained by means of a modified method. Nanostructures ranging from nanowires, nanorods, nanobelts, and nanosheets to dendrites can be obtained. A possible formation mechanism of the nanostructured metal chalcogenides is discussed based on the characterization results.

Results and Discussion

Films of nanostructured copper tellurides: Figure 1 shows a representative X-ray diffraction (XRD) pattern of the resulting copper telluride on copper foil. Apart from the (111)

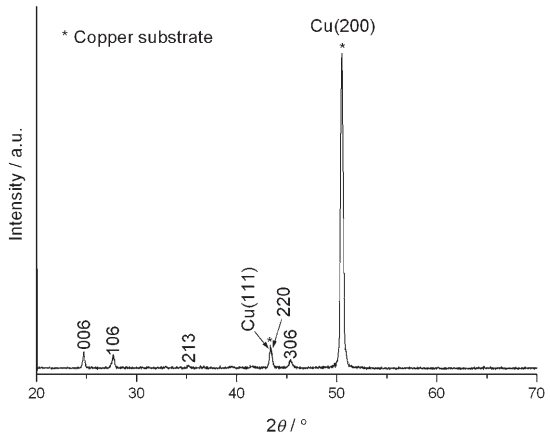

Figure 1. XRD pattern of copper telluride on a copper foil.

and (200) peaks of copper (JCPDS No 04-0836), all of the other peaks can be indexed as (006), (106), (213), (220), and (306) in the hexagonal Cu_2Te structure [space group: $P3m1$ (156)]. The calculated lattice constants $a = 8.3460$ and $c = 21.5932$ Å are in agreement with the standard literature values (JCPDS No. 49-1411). We conclude that the films are composed of pure copper telluride.

The morphology and microstructure of the resulting copper telluride films were investigated by using scanning electron microscopy (SEM). Figure 2 shows that different copper telluride nanostructures were obtained by varying the reaction media. In deionized (DI) water, the resulting film is composed of irregular particles and minor hexagonal plates (Figure 2a). When an aqueous cetyltrimethylammonium bromide (CTAB) solution was used as the reaction media, rodlike structures were obtained (Figure 2b). These

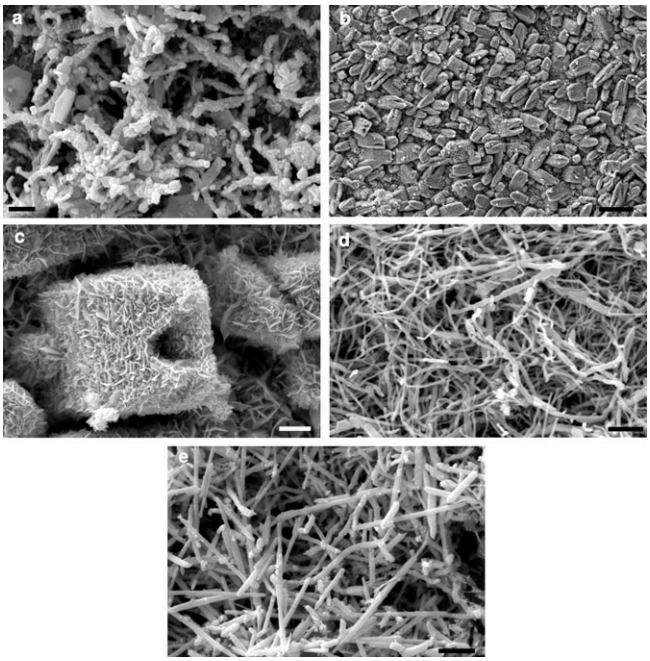

Figure 2. Various copper telluride nanostructures hydrothermally grown in different reaction media: a) DI water, b) and c) an aqueous CTAB solution (1.1 mmol CTAB in 15 mL DI water), d) an aqueous hydrazine solution (1 mL hydrazine in 14 mL DI water), and e) an aqueous mixed CTAB and hydrazine solution (1.1 mmol CTAB and 1 mL hydrazine in 14 mL DI water). The scale bars in a, c, d, and e are 2 μm. The scale bar in b is 10 μm.

micrometer-sized rods possess sharp tips or are hollow inside. A higher magnification SEM image (Figure 2c) reveals that the rods are aggregates of nanosheets. The thickness of the nanosheets is about 50 nm. It is thought that self-assembly of these nanosheets results in the formation of rods. To the best of our knowledge, the synthesis of copper telluride nanosheets and their self-assembly have never previously been reported. When an aqueous hydrazine solution was used as the reaction media, the resulting copper telluride grew into nanowires of more than ten micrometers in length (Figure 2d). The diameters of the nanowires were in the range 50–300 nm. In a mixed CTAB and aqueous hydrazine solution, copper telluride nanorods were formed on the copper foil (Figure 2e). The diameters of the nanorods were in the range 80–400 nm and their lengths were several micrometers. These results indicate that the hydrothermal reaction of copper foils and telluride powders can selectively produce various copper telluride nanostructures through the addition of CTAB and/or hydrazine to water.

The resulting copper telluride nanostructures were further investigated by transmission electron microscopy (TEM). Figure 3 displays the TEM and high-resolution TEM (HRTEM) images of various copper telluride nanostructures hydrothermally grown in different reaction media. Copper telluride nanosheets grown in the CTAB aqueous solution were confirmed by the TEM image displayed in Figure 3a. It was found that the aggregates of nanosheets can be separated by ultrasound while some sheets were destroyed

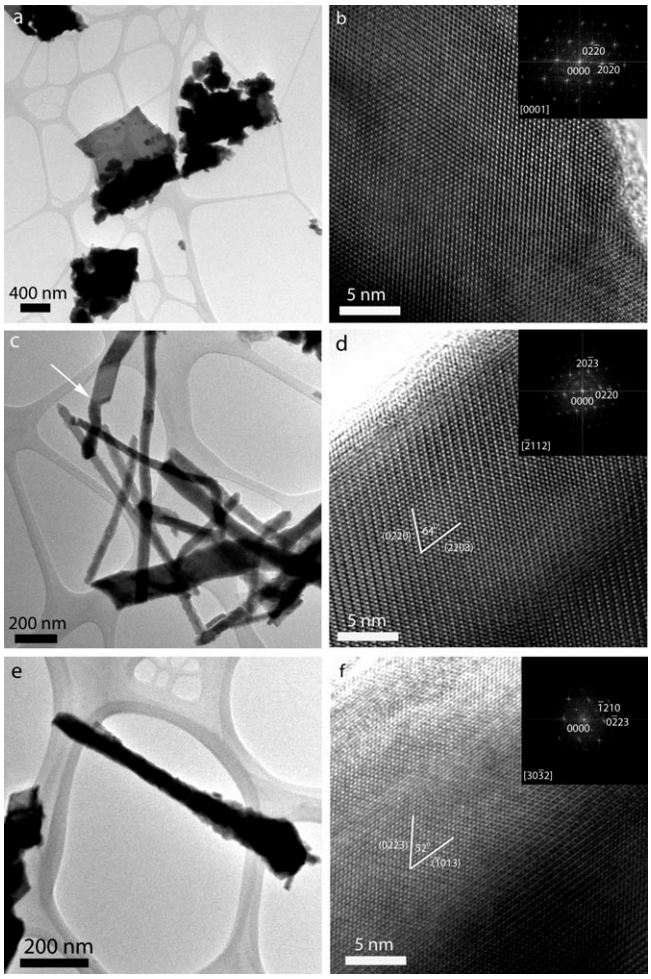

Figure 3. TEM and HRTEM images of various copper telluride nanostructures hydrothermally grown in different reaction media: a and b) an aqueous CTAB solution (1.1 mmol CTAB in 15 mL DI water), c and d) an aqueous hydrazine solution (1 mL hydrazine in 14 mL DI water), and e and f) an aqueous mixed CTAB and hydrazine solution (1.1 mmol CTAB and 1 mL hydrazine in 14 mL DI water). The insets in b, d, and f show the two-dimensional Fourier transform patterns of the corresponding HRTEM images.

during the TEM sample preparation. Figure 3b reveals the single-crystalline nature of the nanosheets, free of dislocation and stacking faults. The two-dimensional Fourier transform pattern (inset of Figure 3b) can be indexed to the [0001] zone of hexagonal copper telluride. Figure 3c displays the copper telluride nanowires grown in the aqueous hydrazine solution. Most of the observed nanowires were about 40–50 nm in diameter, but some long sheets (or wide belts) were found, displayed in Figure 3c. This figure clearly shows that the nanostructure is composed of half wire and half sheet (as indicated by the arrow). HRTEM analysis shows that the nanowires were also single crystalline and free of dislocation and stacking faults. The inset of Figure 3d shows the two-dimensional Fourier transform pattern of the HRTEM image, which can be indexed to the $[\bar{2}112]$ zone of hexagonal copper telluride. From these results, we conclude that the nanowires grow along the $(\bar{2}20\bar{3})$ plane. A TEM image of copper telluride nanorods grown in the mixed CTAB and aqueous hydrazine solution is shown in Figure 3e. Figure 3f displays the HRTEM image of a nanorod and its corresponding two-dimensional Fourier transform pattern, which can be indexed to the $[30\bar{3}2]$ zone of hexagonal copper telluride. So, the growing direction of the nanorods can be concluded to be along the $(\bar{1}013)$ plane.

Films of nanostructured silver tellurides: A representative XRD pattern of silver telluride nanostructures on silver foils is shown in Figure 4. Similar to the XRD results of copper telluride on copper, the peaks can be indexed to face-centered cubic Ag (JCPDS No 87-0718) and monoclinic phase of Ag_2Te [Hessite, space group: $P2/n$ (13), JCPDS No. 34-0142]. Therefore, the nanostructured films formed on silver foils are thought to be pure silver telluride.

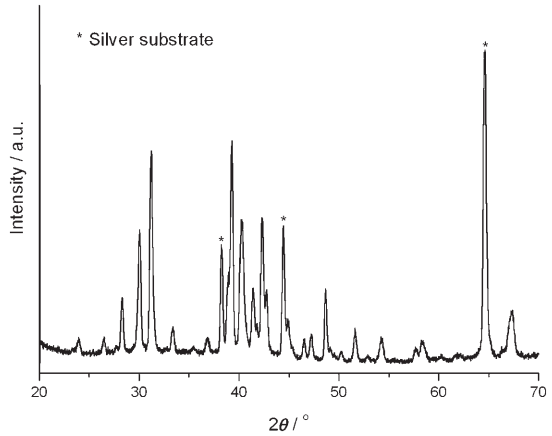

Figure 4. XRD pattern of silver telluride on a silver foil.

Different silver telluride nanostructures are shown in Figure 5. Figure 5a shows that only irregular particles were grown on the silver substrate in DI water. The introduction of CTAB into the system resulted in the formation of nanobelts with a width of about 80 to 200 nm and a length of about a few micrometers (Figure 5b). The rectangle-like cross section of the materials can be observed from the SEM images. Branched and helical nanobelts were also found (indicated by arrows in Figure 5b). In an aqueous hydrazine solution, mostly nanowires and minor nanosheets were obtained (Figure 5c). The resulting nanowires, which were several micrometers in length, were not uniform in diameter. When mixed CTAB and aqueous hydrazine solutions were used as reaction media, two kinds of silver telluride nanostructures (nanowires and hierarchical dendrites) were found on the silver substrate. Nanowires were observed to cover the whole silver substrate in the presence of 2.2 mmol CTAB (Figure 5d). The nanowires possess diameters in the range ~50–300 nm with lengths of several micrometers. As apposed to what was observed in the aqueous hydrazine solution, there were no nanosheets found in the nanostructured film when a mixed CTAB and hydrazine sol-

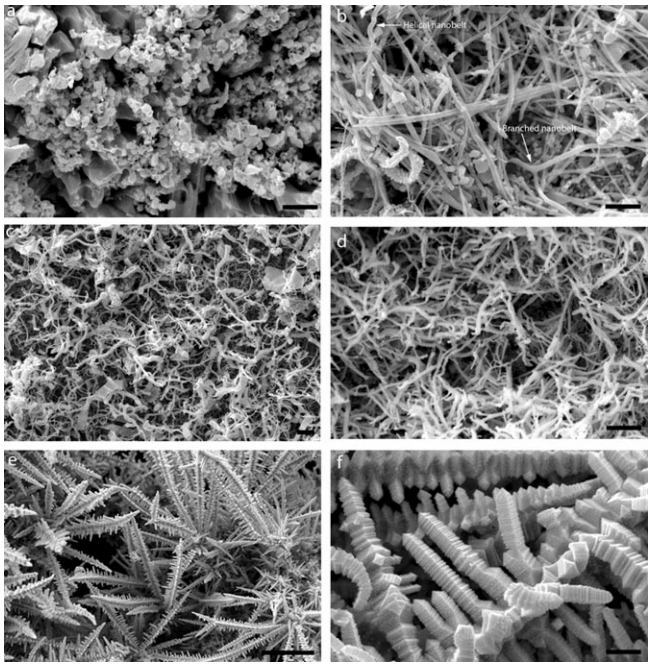

Figure 5. Various silver telluride nanostructures hydrothermally grown in different reaction media: a) DI water; b) an aqueous CTAB solution (2.2 mmol CTAB in 14 mL DI water); c) an aqueous hydrazine solution (1 mL hydrazine in 14 mL DI water); d) an aqueous mixed CTAB and hydrazine solution, in the middle of the foil (2.2 mmol CTAB and 1 mL hydrazine in 14 mL DI water); and e and f) an aqueous mixed CTAB and hydrazine solution, at the edge of the foil (0.1375 mmol CTAB and 1 mL hydrazine in 14 mL DI water). The scale bars in a, b, c, d, and f are 2 μm. The scale bar in e is 10 μm.

ution was used. If the amount of CTAB was decreased to 1/16 of the original concentration (from 2.2 mmol to 0.1375 mmol), nanowires (similar to the wires shown in Figure 5d) grew in the middle part of the silver substrate along with oriented hierarchical dendrites at the edge of the substrates (Figure 5e). The dendritic structures radially grew to form arrays. The individual Ag_2Te dendrites possessed three-dimensional structures with one trunk and four branches. The lengths of the branches were several micrometers and the trunks more than twenty micrometers. The branches were perpendicular to the trunk. Some longer branches were found to possess four side branches similar to the trunk, forming a hierarchical structure (Figure 5f). A higher magnification SEM image also shows that the width of the branches diminishes from bottom to top, forming sharp tips. More interestingly, these towerlike branches were composed of square cross sections, different from the reported dendritic nanostructures of PbS,[23–25] Ag,[26,27] Pt,[28] ZnS,[29] CdS,[30] and so forth. We believe that this is the first report of such hierarchical silver telluride dendrites. This successful controlled synthesis of various silver telluride nanostructures further confirms that our method is a general one for the preparation of nanostructured metal telluride films.

Figure 6 displays TEM and HRTEM images of various silver telluride nanostructures hydrothermally grown in different reaction media. Figure 6a displays the beltlike structure of silver telluride grown in the aqueous CTAB solution. The nanobelt shown is about 70 nm in width. Figure 6b shows that the nanobelt is single crystalline and free of stacking faults. The two-dimensional Fourier transform pattern of the HRTEM image (inset of Figure 6b) can be in-

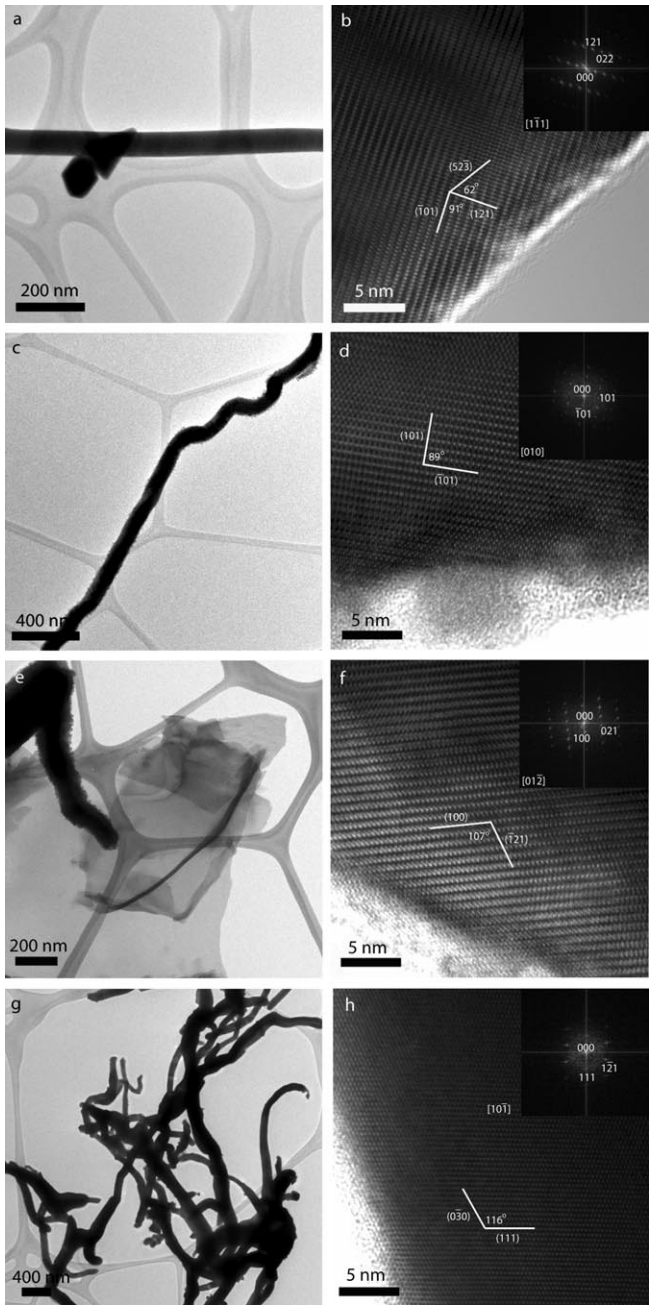

Figure 6. TEM and HRTEM images of various silver telluride nanostructures hydrothermally grown in different reaction media: a) DI water; b) an aqueous CTAB solution (2.2 mmol CTAB in 14 mL DI water); c, d, e, f) an aqueous hydrazine solution (1 mL hydrazine in 14 mL DI water); g and h) an aqueous mixed CTAB and hydrazine solution (2.2 mmol CTAB and 1 mL hydrazine in 14 mL DI water). The insets in b, d, f, and h show the two-dimensional Fourier transform patterns of the corresponding HRTEM images.

dexed to the [$\bar{1}$11] zone of monoclinic silver telluride. The growth direction of the nanobelt was concluded to be along the (52$\bar{3}$) plane. Besides the normal nanowires, an interesting nanowire with a helical part is observed in the silver telluride nanostructures grown in the aqueous hydrazine solution (Figure 6c). This nanowire is also single crystalline and grows along the ($\bar{1}$01) plane, as concluded from HRTEM and a two-dimensional Fourier transform pattern of the HRTEM image, which was indexed to the [010] zone of monoclinic silver telluride (Figure 6d). The coexistence of nanosheets and nanowires in the sample grown in the aqueous hydrazine solution was confirmed through the image displayed in Figure 6e. More importantly, it can be seen that there is a nanosheet partially folded on one side of the image. This observation provides direct evidence for the mechanism of hydrothermally driven rolling up of nanosheets to form one-dimensional metal telluride nanosturtures, proposed in our previous study.[22] HRTEM analysis shows that the nanosheets are single crystalline. The two-dimensional Fourier transform pattern of the HRTEM image (inset of Figure 6f) can be indexed to the [01$\bar{2}$] zone of monoclinic silver telluride. In the aqueous mixed CTAB and hydrazine solution, more abundant nanowires were obtained, as shown in Figure 6g. These nanowires were single crystalline and free of dislocation and stacking faults, as revealed by HRTEM analysis (Figure 6h). The inset of Figure 6h shows the corresponding two-dimensional Fourier transform pattern, which can be indexed to the [10$\bar{1}$] zone of monoclinic silver telluride. It can been concluded that the growing direction of the nanowires is along the (0$\bar{3}$0) plane.

Possible formation mechanism of nanostructured metal tellurides: It is known that natural and artificial lamellar solids can be rolled up into one-dimensional structures (nanotubes and nanowires) under appropriate conditions.[31–34] For nonlamellar solids, Schmidt and Eberl designed a rolling-up approach from a thin solid film to prepare nanotubes; this method relies on the release of thin layers of the materials from a substrate by a selective etching procedure.[35] Similar to the rolling-up mechanism of thin solid films, an in situ hydrothermal rolling mechanism may explain the growth of one-dimensional lead telluride nanostructures on lead foils, described in our previous paper.[22] This mechanism may also be applied to the growth of one-dimensional copper and silver telluride nanostructures based on the characterization results in this study. The first step is the deposition of copper and silver telluride nanofilms on metal foils. However, we believe that this deposition step is different from that of lead telluride films, because copper and silver are not as reactive as lead and therefore active hydrogen could not be produced. We believe that copper and silver metals are first converted into their oxides under hydrothermal reactions;[35] the resulting oxides subsequently react with tellurium powder[36] depositing the corresponding metal tellurides on metal foils. Subsequent in situ hydrothermal rolling of the deposited films then takes place producing the one-dimensional nanostructures.

We found that the geometry of metal foils is crucial for the formation of one-dimensional metal chalcogenides. When metal foils were replaced by metal powders, only irregular particles were obtained.[21,22] So, the foils serve not only as a metal source, but also as a flat platform for the deposition and subsequent wrapping up of metal chalcogenide nanofilms. In this study, aqueous hydrazine and/or CTAB solutions play two roles in the growth of one-dimensional metal chalcogenides. These roles include assisting in the deposition of metal chalcogenide nanofilms and acting as a selective etchant to aid the rolling up of the in situ formed films. One-dimensional metal telluride nanostructures could not be obtained in the absence of both hydrazine and CTAB (Figure 2a and Figure 5a). Moreover, nanostructures composed of half wires and half sheets (Figure 3c) and of half rolling nanosheets (Figure 6e and Figure 7) further confirm that one-dimensional copper and silver tellurides nanostructures are formed through a hydrothermally driven rolling of in situ deposited nanofilms. Furthermore, the single-crystalline nature of the nanosheets (Figure 6e) explains why the subsequently formed one-dimensional nanostructures are single crystalline. This single-crystalline nature represents an attractive advantage of our one-dimensional tellurides compared to those formed by natural, artificial lamellar, and nonlamellar solids.[31–35]

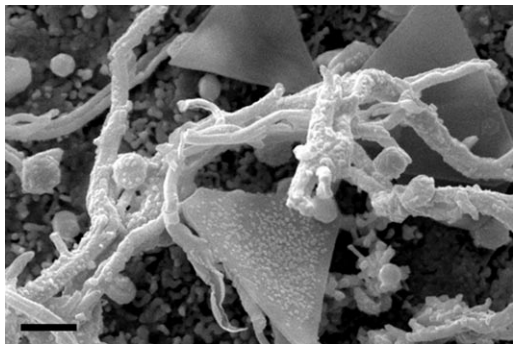

Figure 7. SEM image of nanostructured silver telluride displaying half-rolling nanosheets. The scale bar is 2 μm.

Silver telluride dendrites without one-dimensional shape are found at the silver foil edges (Figure 5e and f). This further proves the importance of the geometry of the metal foils for the formation of one-dimensional metal chalcogenides, because the edge parts cannot provide a flat platform for the deposition and subsequent wrapping up of metal chalcogenide nanofilms. The growth of silver telluride dendrites cannot be explained by the in situ hydrothermal rolling mechanism. It is thought that nonequilibrium growth on the edges of the silver foil would produce the dendrites of silver telluride through oriented aggregation.[37,38]

Conclusions

In this study, various nanostructured copper and silver telluride films on the corresponding metal foils were prepared through hydrothermal reactions between the foils and tellurium powder in different media. Based on the characterization results and our previous studies, the formation of one-dimensional tellurides can be explained by an in situ hydrothermal rolling mechanism. This provides a low-temperature solution-phase method to grow low-dimensional nanostructured metal tellurides with controllable morphologies. The tunable nanostructured telluride films are ideal candidates for studying nanoarchitecture-dependent performance for applications in different fields.

Experimental Section

Synthesis: In a typical procedure, a piece of copper or silver foil (Aldrich, purity: >99.99%, thickness: 0.25 mm, 1.5 cm×0.5 cm, used after rinsing with ethanol), telluride powder (Aldrich, purity: >99.0%, 0.5 mmol), and an appropriate amount of CTAB (Sigma, purity: >99.0%) were placed in a 20 mL Teflon-lined autoclave, and then an aqueous hydrazine solution (6.6% by volume, 15 mL) or DI water (15 mL) was added. The autoclave was maintained at 200°C for 12 h and then air cooled to room temperature. The copper or silver foil was taken out of the solution and washed with ethanol, and finally air dried for characterization.

Characterization: X-ray powder diffraction patterns were obtained on a Bruker D8 Advance X-ray diffractometer with $Cu_{K\alpha}$ radiation (λ = 1.54178 Å). The SEM images and energy-dispersive XRD spectra were performed on a LEO 1450 VP scanning electron microscope with an energy-dispersive XRD instrument. TEM images were recorded on a Tecnai 20 FEG transmission electron microscope.

Acknowledgements

The work described in this paper was partially supported by the National Science Foundation of China (20503009). We thank Dr Z. S. Li (Ecomaterials and Renewable Energy Research Center, Department of Physics, Nanjing University) for his kind help with the HRTEM analysis.

[1] W. Z. Wang, Y. Geng, P. Yan, F. Y. Liu, Y. Xie, Y. T. Qian, *J. Am. Chem. Soc.* **1999**, *121*, 4062.
[2] Y. Li, Y. Ding, Y. T. Qian, Y. Zhang, L. Yang, *Inorg. Chem.* **1998**, *37*, 2844.
[3] K. Sridhar, K. Chattopadhyay, *J. Alloys Compd.* **1998**, *264*, 293.
[4] M. Kobayashi, K. Ishikawa, F. Tachibana, H. Okazaki, *Phys. Rev. B* **1988**, *38*, 3050.
[5] R. Xu, A. Husmann, T. F. Rosenbaum, M. L. Saboungi, *Nature* **1997**, *390*, 57.
[6] H. S. Schnyders, M. L. Saboungi, T. F. Rosenbaum, *Appl. Phys. Lett.* **2000**, *76*, 1710.
[7] I. S. Chuprakov, K. H. Dahmen, *Appl. Phys. Lett.* **1998**, *72*, 2165.
[8] C. Nascu, I. Pop, V. Ionscu, E. Indra, I. Bratu, *Mater. Lett.* **1997**, *32*, 73.
[9] M. A. Korzhuev, *Phys. Solid State* **1998**, *40*, 217.
[10] H. M. Pathan, C. D. Lokhande, D. P. Amalnerkar, T. Seth, *Appl. Surf. Sci.* **2003**, *218*, 290.
[11] R. Coustal, *J. Chim. Phys.* **1958**, *38*, 277.
[12] C. J. Warren, R. C. Haushalter, A. B. Bocarsly, *J. Alloys Compd.* **1995**, *229*, 175.
[13] K. Sridhar, K. Chattopadhyay, *J. Alloys Compd.* **1998**, *264*, 293.
[14] G. Henshaw, I. P. Parkin, G. Shaw, *Chem. Commun.* **1996**, 1095.
[15] G. Henshaw, I. P. Parkin, G. Shaw, *J. Chem. Soc., Dalton Trans.* **1997**, 231.
[16] W. Z. Wang, P. Yan, F. Y. Liu, Y. Xie, Y. Geng, Y. T. Qian, *J. Mater. Chem.* **1998**, *8*, 2321.
[17] S. H. Yu, Z. H. Han, J. Yang, R. Y. Yang, Y. Xie, Y. T. Qian, *Chem. Lett.* **1998**, 1111.
[18] Y. Xie, L. Y. Zhu, X. C. Jiang, J. Lu, X. W. Zheng, W. He, Y. Z. Li, *Chem. Mater.* **2001**, *13*, 3927.
[19] R. Z. Chen, D. S. Xu, G. L. Guo, L. L. Gui, *J. Mater. Chem.* **2002**, *12*, 2435.
[20] R. Z. Chen, D. S. Xu, G. L. Guo, Y. Q. Tang, *Chem. Phys. Lett.* **2003**, *377*, 205.
[21] L. Z. Zhang, J. C. Yu, M. S. Mo, L. Wu, Q. Li, K. W. Kwong, *J. Am. Chem. Soc.* **2004**, *126*, 8116.
[22] L. Z. Zhang, J. C. Yu, M. S. Mo, L. Wu, Q. Li, K. W. Kwong, *Small* **2005**, *1*, 349.
[23] D. B. Kuang, A. W. Xu, Y. P. Fang, H. Q. Liu, C. Frommen, D. Fenske, *Adv. Mater.* **2003**, *15*, 1747.
[24] D. B. Wang, D. B. Yu, M. W. Shao, X. M. Liu, W. C. Yu, Y. T. Qian, *J. Cryst. Growth* **2003**, *257*, 384.
[25] Y. R. Ma, L. M. Qi, J. M. Ma, H. M. Cheng, *Cryst. Growth Des.* **2004**, *4*, 351.
[26] G. J. Lee, S. I. Shin, S. G. Oh, *Chem. Lett.* **2004**, *33*, 118.
[27] R. He, X. F. Qian, J. Yin, Z. K. Zhu, *Chem. Phys. Lett.* **2003**, *369*, 454.
[28] Y. J. Song, Y. Yang, C. J. Medforth, E. Pereira, A. K. Singh, H. F. Xu, Y. B. Jiang, C. J. Brinker, F. van Swol, J. A. Shelnutt, *J. Am. Chem. Soc.* **2004**, *126*, 635.
[29] Y. C. Zhu, Y. Bando, L. W. Yin, *Adv. Mater.* **2004**, *16*, 331.
[30] L. F. Dong, T. Gushtyuk, J. Jiao, *J. Phys. Chem. B* **2004**, *108*, 1617.
[31] R. E. Schaak, T. E. Mallouk, *Chem. Mater.* **2000**, *12*, 3427.
[32] Y. D. Li, X. L. Li, R. R. He, J. Zhu, Z. X. Deng, *J. Am. Chem. Soc.* **2002**, *124*, 1411.
[33] X. Chen, X. Sun, Y. Li, *Inorg. Chem.* **2002**, *41*, 4524.
[34] Y. J. Xiong, Y. Xie, Z. Q. Li, X. X. Li, S. M. Gao, *Chem. Eur. J.* **2004**, *10*, 654.
[35] O. G. Schmidt, K. Eberl, *Nature* **2001**, *410*, 168.
[36] X. Jiang, B. Xie, J. Wu, S. W. Yuan, Y. Wu, H. Huang, Y. T. Qian, *J. Solid State Chem.* **2002**, *167*, 28.
[37] M. S. Mo, Z. Y. Zhu, X. G. Yang, X. Y. Liu, S. Y. Zhang, J. Gao, Y. T. Qian, *J. Cryst. Growth* **2003**, *256*, 377.
[38] H. M. Hu, B. J. Yang, Q. W. Li, X. Y. Liu, W. C. Yu, Y. T. Qian, *J. Cryst. Growth* **2004**, *261*, 485.

Received: November 11, 2005
Published online: March 7, 2006

